Solubility of Hydrogen in PdAg and PdAu Binary Alloys Using Density Functional Theory

Chandrashekhar G. Sonwane, Jennifer Wilcox,* and Yi Hua Ma

Department of Chemical Engineering, Worcester Polytechnic Institute, Worcester, Massachusetts 01609

Received: July 16, 2006; In Final Form: September 30, 2006

The present work deals with the study of palladium-silver (PdAg) and palladium-gold (PdAu) binary alloys over a broad range of temperatures and alloy compositions using density functional theory (DFT) to find possible conditions where the solubility of hydrogen (H) is significantly higher than that of pure palladium (Pd). Several alloy structures, such as $Pd_{100-x}Ag_x$ with $x = 14.81$, 25.93, 37.04, and 48.51, $Pd_{100-x}Au_x$ with $x = 14.81$, 25.93, and 37.04, and $Pd_{100-x}Cu_x$ with $x = 25.93$ and 48.51 were considered. The lattice constants of these structures were optimized using DFT, and relaxed structures were used for the estimation of binding energy. It was found that the solubility of H in PdAg is higher than pure Pd with a maximum at approximately 30% Ag at 456 K. Also, the solubility of PdAu alloys was higher than pure Pd with a maximum at about 20% Au with a solubility 12 times higher than that of pure Pd. It was found that for a 3.7% H concentration in a PdAg alloy, a cell expansion of 0.15−0.2% occurs, which if ignored may affect the individual binding energy of the O-site by approximately 3.56% and may affect the predicted solubility by approximately 11.8%.

Introduction

The gradually increasing oil consumption and the political instabilities in the oil-producing nations have led to rising fuel prices. These factors along with the need for environmentally friendly energy sources (with no pollution or low pollution) have raised the importance of hydrogen (H) as a fuel for future energy. At present, H is primarily used in ammonia manufacturing, petroleum refining, methanol synthesis, fuel for space shuttles, and fuel cells that provide heat, electricity, and drinking water for astronauts. In the future, H could be used to fuel vehicles and aircrafts and to provide power to our home and offices. The challenges for producing pure H at lower cost requires the fabrication of very thin, high-permeability Pd-based membranes that are stable at high temperature and pressures for the long operation times typically employed in petrochemical industries. However, for pure Pd membranes, the loading and unloading of H during the operation of membrane reactors causes expansion and contraction of the lattice due to $\alpha \leftrightarrow \beta$ phase transformations,[1] making the membrane vulnerable to embrittlement. Several experimental reports suggest that alloying Pd with other metals such as Ag, Au, or Cu helps by reducing the embrittlement, offering resistance to poisoning, and providing a longer operational lifetime, which are important for reducing the cost of producing H. Alloying Pd with these metals suppresses the critical point of $\alpha \leftrightarrow \beta$ phase transformations. The PdCu alloy has been found to be tolerant to sulfur poisoning,[2−4] however it has significantly lower hydrogen solubility (as well as permeability) as compared to pure Pd. In the first attempts, in 1869, Graham[5] suggested that PdAg alloys have higher H solubility as compared to pure Pd. Later, Gryaznov[6] also suggested that the permeability of H in PdAg is higher than that in pure Pd. Experiments in the past have shown that 23−32% Ag in a PdAg alloy has significantly higher solubility[7] and permeability[6,7] as compared to pure Pd. The addition of Ag reduces the critical temperature of $\alpha \leftrightarrow \beta$ phase transformations, and also increases the solubility of H, while simultaneously reducing its diffusion coefficient, causing an increased H permeability. Amandusson et al.[8] found that PdAg alloy with 32% Ag at 623 K has 6 times higher permeability as compared to pure Pd. In addition, the PdAg alloy with compositions greater than 30% Ag does not have $\alpha \leftrightarrow \beta$ phase transformations occurring at low temperatures, which is a major cause of defects in membranes. The addition of Cu causes contraction of the Pd cell while the addition of Ag or Au causes cell expansion. It has been hypothesized that by providing an expanded lattice, that is, PdAg or PdAu, one can avoid the expansion/contractions, thereby reducing the embrittlement of the membrane due to limiting the $\alpha \leftrightarrow \beta$ phase transformations.[9]

The molecular simulation work performed in the past, related to the solubility of H in PdAg and PdAu, has not taken into account the random ordering of atoms in periodic supercells. Instead, these approaches have used the approximation of representing the PdAg alloy as a cluster of 4 atoms in a face-centered cubic (fcc) arrangement with or without periodic boundary conditions. A system and approach used by these researchers[10−13] does not provide the flexibility of estimating binding energy as well as solubility of PdAg and PdAu alloys with intermediate alloy compositions, hydrogen concentrations, and operating conditions (temperature, pressure) to find a suitable system composition and operating conditions for higher solubility. In addition, the errors associated with neglecting the effect of lattice expansion due to H on the binding energy/solubility are completely ignored under the assumption that they are negligible. Although there have been attempts to estimate the absorption energy and use that as a tool to hypothesize the trend in solubility (without providing quantitative estimates), there have been no attempts to predict the solubility of PdAg as well as PdAu alloys by ab initio simulations and compare with experiments or to lead experimentalists to design efficient membranes. The main goals of the present work involve the use of density functional theory (DFT) based simulation techniques reported by Kamakoti et al.,[2−4] validating them with experimental results for pure Pd and the CuPd binary alloy,

* To whom correspondence should be addressed. Tel: 508-831-5493. Fax: 508-831-5853. E-mail: jwilcox@wpi.edu.

10.1021/jp064507t CCC: $33.50
Published on Web 11/11/2006

extending it to examine the solubility of H in PdAg and PdAu systems, and comparing them with the experimental results. The local alloy composition, that is, the nearest and next nearest neighbors, NN and NNN, respectively, was changed to obtain a nonlinear dependency of binding energy as a function of NN, NNN, and the lattice constant of the alloy. The binding energy was then used to obtain the solubility and $P-T$ relationship over a temperature range of 400−1200 K.

Theoretical Procedure

Pure Pd and its alloys were simulated as three-dimensional (3D) infinite periodic structures by defining a supercell and periodic boundary conditions in all three principal axes. All the simulations were carried out using Vienna ab initio Simulation Package (VASP).[14,15] The electron exchange correlation effects were described by a generalized gradient approximation (GGA) using the Perdew−Wang 91 functional. A plane wave expansion with a cutoff 199 eV was used in all of the calculations for Pd, PdAg, and PdAu alloys while 234 eV was used for PdCu alloys. The variation of the cutoff potential changes the individual energy of the supercells by a small magnitude, but the binding energy which is obtained by subtracting the energy of supercells with and without hydrogen, the effect of varying the cutoff potential, is less than 3%. The total *energy* calculations used the residual minimization method for electronic relaxation and accelerated the calculations using the Methfessel−Paxton Fermi-level smearing with a width of 0.2 eV. Geometry relaxation calculations employed the conjugate-gradient (CG) algorithm until the forces on the unconstrained atoms were less than 0.03 eV/Å. A Monkhorst-Pack mesh with a 4 × 4 × 4 k-grid was used for all the simulations involving Pd, PdAg, and PdAu alloys. The normal mode vibrational frequencies were estimated for the Born−Oppenheimer potential energy surface from the second derivative matrix, that is, the Hessian, using a small H-atom displacement of 0.15 Å. The displacement was small enough to assume a harmonic potential and sufficient enough to produce an energy difference relative to the energy minima to be calculated accurately. Ke and Kramer[12] used a four-atom system with Pd and Ag atoms and with periodic boundary conditions. Using DFT, they reported that there is a significant difference between the anharmonic and harmonic potentials. They used the ANHARMND package which solves the time-dependent Schrödinger wave equation, by fitting a polynomial function to the potential energy surface, and they found that a harmonic approximation is inadequate for studying the vibrations of H in PdAg alloys. The H concentration used in their system was 25%, which is significantly higher than that used in the present work (3.7%). Such a higher concentration of H leads to an expanded cell which is also known to affect the vibrational frequencies.[12] In the present work, the approach presented by Kamakoti et al.[4] was used, where the displacement of H atoms was small enough to have a reasonable harmonic assumption. In the future, it may be worthwhile to investigate the anharmonic potential for H vibrations in the supercell in which concentration of H is 3.7% to validate our assumption.

The experimental results in the literature suggest that H spends a considerable amount of time at the O-sites as compared to the T-sites. Rowe et al.[16] studied the diffusion of H in a single crystal of Pd at 3% H concentration using quasielastic neutron scattering and found that H is predominantly present on the O-sites and that diffusion occurs by simple jumps between adjacent O-sites. Nelin and Skold[17,18] also used quasielastic neutron scattering to study the diffusion of H in Pd in both α- and β-phases. They found that the hydrogen diffusion mechanism in both phases is the same and that the jumps occur between adjacent O-sites. Worsham et al.[19] used H and deuterium in Pd in β-phases and found that protons of H in Pd are more nearly free than in other H compounds. In addition, Gillan[9] using MD simulations indicated that the residence time of an H atom at an O-site in a Pd fcc lattice was significantly higher than that of the T-site and that the motion of H could be approximated as hops through O−T−O sites. In the present work, the binding energies of O- as well as T-sites have been estimated using $E_b = E_{SS+H} - E_{SS} - (1/2)E_{H2}$ where SS represents the supercell. A schematic of O-, T-, and TS-sites is shown in Figure 1. For the simulation of the lattice constants, binding energies, and solubility, 3 × 3 × 3 supercells were used with the atoms placed upon an fcc structure with principal axes along the faces of the cubic unit. Developing a pure Pd supercell is fairly straightforward since all the atoms on the fcc lattice are the same so that the structure can be replicated in all three directions with minimal complications. However, for PdAg and PdAu alloys, several factors needed to be considered such as (a) the phase diagram and crystal structure, (b) statistics for short and long range ordering of alloy atoms, and (c) the availability of computational resources. Increasing the size of the supercell allows for statistical improvement, but it also increases the computational time required. A balance can be achieved by extending the method of Kamakoti et al.,[2−4] in which the information from a smaller supercell is used to obtain the O-site binding energies (or T-site, TS energy, etc.) which relate the DFT energy to the local alloy atomic composition, that is, nearest neighbor (NN) and next nearest neighbor (NNN) of the alloying atom. The binding energies obtained by such a method can then be used to study a larger alloy system.

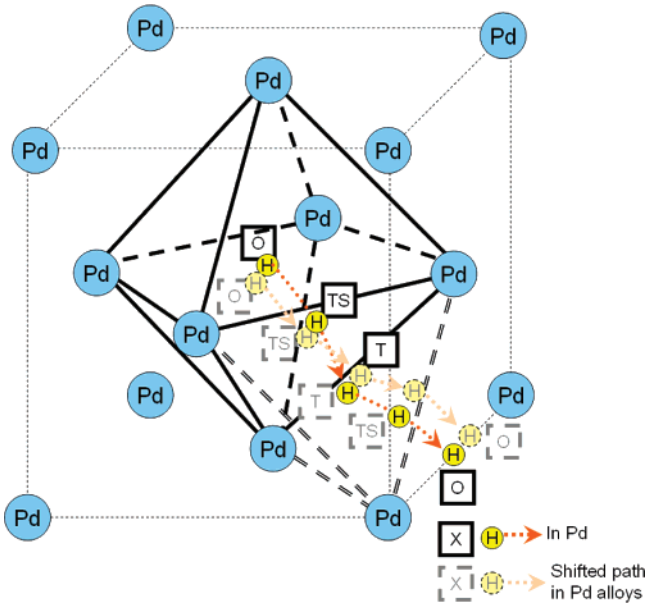

Figure 1. Schematic of O-, T-, and TS-sites in a palladium lattice.

The method of simulating H diffusion in Pd alloys, for example, PdAg and PdAu, is more complex than that of pure Pd. The first step is to simulate an accurate structure of a given Pd alloy with regard to the relative arrangement of Pd and Ag (or Au) atoms in the lattice and the type of crystal lattice from which these atoms are distributed. The information of the crystal lattice can be obtained from the phase diagrams available in the literature.[20] In the present work, the PdAg and PdAu systems were modeled as completely miscible fcc crystal structures. The phase diagram of PdAg[20] is a continuous miscible structure over the entire composition and temperature range considered. The

PdAu system[20] is a miscible fcc structure except for a narrow range of composition and temperature. Specifically, between 13 and 30% and 70−80% of Pd in a PdAu alloy (in 873−1073 K) and 43−55% Pd (in 293−363 K) in a PdAu alloy may have a cubic structure or other unknown structures (not fcc). However, due to the uncertainty in knowing the details of the structure at these different composition/temperature conditions, a uniform approach involving strictly fcc structures had to be considered in the present work. In the present work, for the simulation of solubility, a 13 × 13 × 13 structure has been used. A supercell with 27 atoms was used to estimate the dependence of binding energy on the nearest neighbors, next nearest neighbors, and the lattice constant. For each alloy composition, the position of Pd and Ag atoms was changed such that several combinations of NN (minimum 0, maximum 6) and NNN (minimum 0, maximum 8) referring to the number of Ag (or Au) atoms were assumed. Alloy compositions of $Pd_{100-x}Ag_x$ with $x = 14.81$, 25.93, 37.04, and 48.51, $Pd_{100-x}Au_x$ with $x = 14.81$, 25.93, and 37.04, and $Pd_{100-x}Cu_x$ with $x = 25.93$ and 48.51 were examined. The mole percent shown here is obtained by dividing the number of alloying atoms from the total number of atoms in the supercell. A nonlinear equation was used to obtain a predicted binding energy with NN, NNN, and lattice constant as independent variables. This was later used on a larger 13 × 13 × 13 structure to estimate the binding energy at each individual site.

The solubility was estimated using $\theta = K_S P_{H2}^{1/2}$ where θ is the solubility, K_S is Sievert's constant, and P_{H2} is the H pressure in the gas phase. Sievert's constant was estimated using eq i,[21,22]

$$K_s = \exp\left(\beta\left[-\frac{D_E}{2} + \frac{h\nu_{H2}}{4} - E_O - \frac{3}{2}h\nu_H\right]\right)\frac{1}{\sqrt{\alpha}} \sqrt{1 - \exp(-\beta h\nu_{H2}/2)}\frac{1}{(1 - e^{-\beta h\nu_H})} \quad \text{(i)}$$

where

$$\alpha = \left(\frac{2\pi mkT}{h^2}\right)^{3/2}\frac{4\pi^2 I(kT)^2}{h^2}$$

and $\beta = 1/k_BT$, k_B is Boltzmann's constant, D_E is the classical dissociation energy, E_O is the binding energy, h is Planck's constant, I is the molecular moment of inertia, ν_H and ν_{H2} are vibrational frequency of H in the Pd and gaseous states, respectively, and m is the mass of the H molecule.

Results and Discussion

1. Lattice Constant of Pd−H System. The lattice constant of pure Pd obtained by DFT was found to be 3.96 Å. It is higher than the experimental value of 3.89 Å[23] by 1.7% and close to the simulated value of 3.95 Å reported by Kamakoti et al.[3,4] In the present work, we compare our simulations with the actual experimental values (at 20 °C) instead of the extrapolated values at 0 K estimated using the coefficient of thermal expansion. The errors could vary by 0−2% if estimates at 0 K are taken. In the past, the majority of simulations have ignored the expansion of the Pd lattice due to the addition of H by suggesting that it is negligible. Later, when the binding energy and solubility are discussed, we will show that even for a dilute concentration of H, that is, 3.7% H in Pd alloys, the predicted binding energies are higher by 3.56% and eventually the solubility is underpredicted by about 11.8%. We have attempted to investigate the lattice expansion due to the addition of H over a broad range of H concentrations. For this purpose, an H atom was placed at a randomly selected O-site. Depending upon the concentration of H desired, additional H atoms were placed on the available O-sites. The optimum cell constant as a function of H concentration (H/M, the atoms of H per atom of metal) obtained in the present work is compared with the experimental results[24] at 298 K as shown in Figure 2. The average error in predicting the experimental lattice constants for Pd with H over a broad range of H concentrations is approximately 1.5%.

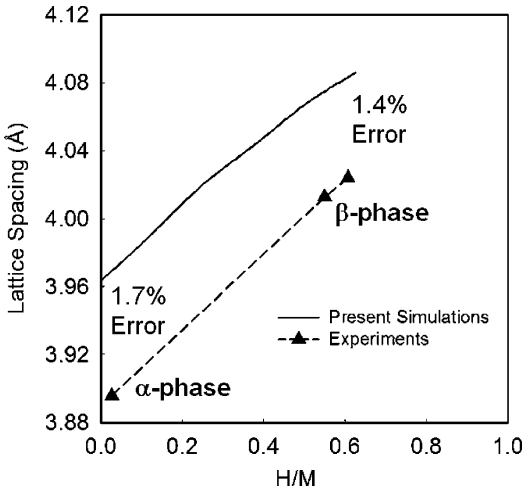

Figure 2. Lattice spacing of pure Pd as a function of the H concentration. H/M corresponds to the molar ratio of H to Pd. Experimental data taken from Mealand and Flanagan.[21]

At low temperatures, the H present in Pd can have two different phases, that is, α and β, depending upon the concentration of H in Pd, with each phase having significantly different lattice constants. In addition, some researchers have claimed that the absorption of H may occur at the T-site along with the O-site in the β-phase. It should be noted that the experimental and simulation results in the literature show that, at low concentration of H (corresponding to the α phase) in Pd, the H atoms are predominantly present at the O-sites. At low temperatures, a change in H concentration in Pd can lead to α ↔ β phase transitions with a sudden change in lattice spacing. The lattice expansion can cause embrittlement in the Pd membranes, therefore reducing its selectivity for H separation. In addition, the H permeabilities are considerably low at lower temperatures. To avoid the problems of membrane embrittlement and low permeabilities, the H separation is carried out at higher temperatures through Pd alloy membranes. Alloying Pd with other metals suppresses the critical temperature of phase transition, enabling high selectivity of H separation at lower temperatures.[1]

2. Lattice Constant of PdAg, PdAu, and PdCu. For the purpose of estimating the lattice constant of each alloy examined, Pd with 0%, 14.81%, 25.93%, 37.04%, 48.15%, and 100% alloying atom, that is, Ag or Au were studied in the present work. The estimates of the lattice constant of these six systems were used to determine the lattice constant of any alloy with intermediate alloy composition between 0 and 100%. The optimum cell constant of the PdAg with and without absorbed H is compared with the experimental data[20] as shown in Table 1. The simulated lattice spacing of the PdAg alloy in the present work matches closely with that of the simulated lattice spacing of Løvvik and Olsen.[13] It can be seen from Table 1 that the simulated lattice spacing of alloys without H atoms is approximately 0.08 Å, which corresponds to a 2−3% deviation from the experimental data. The experimental values reported

TABLE 1: Lattice Constant (*a*) of PdAg and PdAu Alloys without H

X, mol % M in PdM, (M = Ag or Au)	PdAg alloy			PdAu alloy		
	predictions (Å)	experimenta (Å)	% error	predictions (Å)	experiment[a] (Å)	% error
0	3.960	3.883	1.94	3.960	3.883	1.94
14.8	3.989	3.909	2.01	3.997	3.911	2.15
25.9	4.010	3.928	2.04	4.022	3.932	2.24
37.0	4.030	3.947	2.06	4.046	3.952	2.32
48.2	4.049	3.967	2.03	4.069	3.972	2.38

[a] For PdAg, experimental[21] lattice constant, *a*, vs mole percent, *X*, data was fitted to the polynomials, $a = 3.883 + 0.001744X - 0.00000169X^2 + 0.00000003748X^3$ ($r^2 = 0.999$) and for PdAu, $a = 3.883 + 0.00196X - 0.000003706X^2 + 0.00000002877X^3$ ($r^2 = 0.999$).

TABLE 2: Expansion of PdAg Alloy Lattice with Dilute H Concentrations

Ag in PdAg alloy (mol %)	predicted lattice spacing (Å) without H	predicted lattice spacing (Å) with 3.7% H	expansion of PdAg lattice by addition of H (%)
0	3.954	3.960	0.15
14.8	3.989	3.998	0.23
25.9	4.010	4.018	0.20
37.0	4.030	4.038	0.20
48.2	4.049	4.058	0.22

TABLE 3: Expansion of PdAu Alloy Lattice with Dilute H Concentrations

Au in PdAu alloy (mol %)	predicted lattice spacing (Å) without H	predicted lattice spacing (Å) with 3.7% H	expansion of PdAu lattice by addition of H (%)
0	3.954	3.960	0.15
14.8	3.997	4.005	0.20
25.9	4.022	4.029	0.17
37.0	4.046	4.052	0.15
48.2	4.069	4.075	0.15

in Table 1 are obtained by substituting the particular alloy composition studied into a polynomial fitted to the experimental lattice constant data.[20] For the same alloy composition, the lattice constant of PdAu is greater than that of PdAg. Traditionally, the approximate lattice constant of a binary alloy is estimated from the mole fraction and the lattice spacing of its individual metals using Vegard's law. This suggests that the solubility of an alloy is a linear combination of lattice spacing of the individual metal components and their mole fraction as given by eq ii,

$$a_{PdM} = x_M a_M + (1 - x_M) a_{Pd} \qquad \text{(ii)}$$

In eq ii, M refers to the alloying atom, for example, Au or Ag, *a* is the lattice constant, and *x* is the mole fraction. Through the use of the lattice constant of pure Pd and that of the alloying atom, the lattice constant of the remainder of the alloy compositions between 0 and 100 can be estimated using Vegard's law.[3] By the use of the simulated lattice spacing of Pd, Ag, and Au, Vegard's law was used to predict the lattice constant of PdAg or PdAu alloys with 14.81%, 25.93%, 37.04%, and 48.15% alloying metal, and it was found that the predictions are close to the simulated lattice constant. The expansion effect of adding H (3.7%) to the lattice constant of a PdAg system is shown in Table 2. It can be seen that for the 0−48.2% range, the lattice expansion is about 0.2−0.25%. The cell expansion for the PdAu system over an alloy composition of 0−48.2% was found to be about 0.15−0.2% as shown in Table 3. Although these values appear to be small, it will be shown later that they make a significant difference in the binding energy and the predicted solubility of H in Pd-based alloys.

For the PdCu system, only two systems have been considered, that is, 25.93% and 48.15% Cu in PdCu alloy. This was done to verify the procedure used in the present work by comparing the results to those of Kamakoti et al.[3,4] who have used the same system. The lattice constants of these two systems without H were found to be 3.895 and 3.833 Å, respectively. The values with 3.7mol % of H were found to be 3.886 Å and 3.826 Å, respectively. The cell expansion in these systems by the addition of H is about 0.23% and 0.18%, respectively. The simulated cell constant for a 48.15% Cu alloy is 3.77 Å, suggesting an error of 1.64%. The lattice constant for pure Cu and without H was found to be 3.643 Å, which is close to the experimental value of 3.61 Å, with an error of 0.9%. Vegard's law does very well in predicting the alloy composition of the PdAu system, however, it shows small deviations (<0.5%) for the prediction of the lattice spacing for PdAg alloys. The lattice expansion of PdAg and PdAu alloys with the addition of H over hydrogen to metal ratio from 0 to 1 was also studied. It was found that the lattice expansion occurs similar to that of pure Pd, which contradicts some of the explanations offered by experimentalists[8] for H embrittlement. It was suggested in the literature that an already expanded lattice of PdAg alloys (compared to pure Pd) prevents further expansion due to addition of H atoms reducing the possibility of embrittlement. It was found that the lattice expands due to the addition of H for both pure Pd as well as Pd alloys.

3. Binding Energy. The binding energy of H at the O- and T-sites (E_O and E_T) as a function of local alloy composition has been estimated. The H-atom was placed at one O- or T-site and the number of nearest neighbors (NN) and next nearest neighbor (NNN) atoms were varied. For an O-site, 0 < NN < 6 and 0 < NNN < 8 while for a T-site, 0 < NN < 4 and 0 < NNN < 12, which represents the number of alloying atom (Ag, Au, or Cu) with possible values between 0 and 6, with the remainder of the nearest and next nearest atoms being Pd. For a pure Pd system, E_O and E_T were found to be −0.11 and −0.058 eV, respectively. If the binding energy of a site is lower, it tends to have a higher affinity for H and is considered to be an energetically favorable site. The binding energies of several alloys (PdAg, PdAu, and PdCu) are shown in Figures 3−6. The H-binding energies at the O- and T-sites for the PdAg alloy with no Ag atoms in the NN or NNN shell, that is, NN = 0 and NNN = 0, for several alloy compositions studied in the present work are shown in Figure 3a. The purpose of these bar graph plots is to gain further understanding of the H-binding mechanism between the O- and T-sites. The 3D plots in Figures 4−6 provide an interpretation of the overall trend that exists in the binding energies at the O-site as a function of NN and NNN over an entire range alloy compositions. Figure 3a shows that the binding energy at the O-site is less than that at the T-site for pure Pd and at 14.81% Ag. However, at 25.93% Ag, the binding energies at the O- and T-site are almost equal. For 37.04% and 48.15% Ag, the binding energy at the T-site is less than that at the O-site. As the percentage of Ag in the alloy increases, the difference between T-site and O-site energy increases. This suggests that with NN = 0, NNN = 0, and PdAg

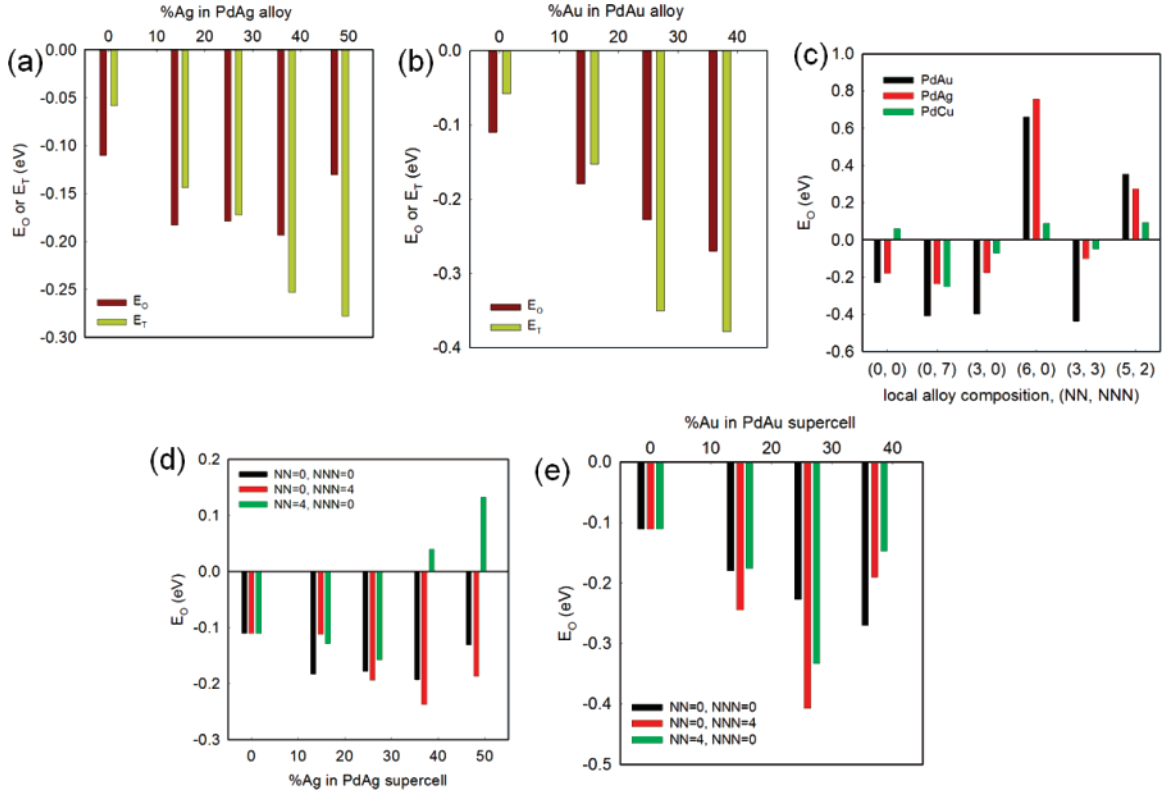

Figure 3. Binding energy of O-sites as a function of the local alloy composition, (a) O- and T-site binding energies for PdAg and (b) PdAu alloys, (c) O-site binding energies for PdAg, PdAu, and PdCu for 25.93% alloying metal, and O-site binding energy of PdAg (d) and PdAu (e) alloys for three specific alloy local compositions, that is, NN = 0 and NNN = 0; NN = 0 and NNN = 4; NN = 4 and NNN = 0.

greater than or equal to 25.93% Ag, the T-site is energetically more favorable compared to the O-site. A similar plot for the PdAu system is shown in Figure 3b. Similarly, for PdAu, with increasing Au, the T-sites become energetically more favorable for the absorption of H. For 14.81% Au, $E_O < E_T$, but for 25.93% and 37.04% Au, $E_O > E_T$, suggesting that the T-sites are energetically favorable for H absorption. These results are consistent with Løvvik and Olsen,[13] who found that when most of the neighbors are palladium atoms, the O-site is a preferred site, while the T-site is preferred when Ag dominates.

A comparison of the O-site binding energy for PdM with 25.93% alloying metal, that is, Ag, Au, or Cu for a series of local alloy compositions, that is, varying NN and NNN, is shown in Figure 3c. For NN = 0 and NNN = 0, the O-site binding energies are $E_O^{PdCu} > E_O^{PdAg} > E_O^{PdAu}$. This suggests that PdAu as well as PdAg provide stronger absorption sites as compared to the PdCu alloy. When the alloying atom, that is, Ag or Au in the NNN shell is increased to NNN = 7, more O-sites in PdCu become energetically favorable. Overall, the PdAg and PdAu alloys provide stronger absorption sites. Increasing alloying atoms in the NN, that is, NN = 3 and NNN = 0 makes the PdAg and PdAu sites stronger but PdCu sites weaker as compared to pure Pd. In all the energetically favorable sites, the PdAu alloy provides the strongest absorption sites. A large increase in M in the nearest neighbor shell, that is, NNN = 0 and NN = 6 makes the sites unfavorable for all three alloys.

The O-site binding energy of the PdAu alloy is lower than that of PdAg and PdCu for local alloy compositions of NN = 0 and NNN = 0; NN = 0 and NNN = 7; NN = 3 and NNN = 0; NN = 3 and NNN = 3, which suggests that PdAu provides stronger H-binding sites compared to PdAg and PdCu alloys. The O-site binding energy alloys with NN = 6 and NNN = 0 as well as NN = 5 and NNN = 2 are positive suggesting that these are energetically not favorable for H absorption. At NN = 0 and NNN = 7, the O-site binding energy for PdAg is lower than that for PdCu suggesting that H binding in PdAg is favorable. The results suggest that increasing alloying atoms in the next nearest neighbor is favorable for absorption of H. However, for nearest neighbors, it is favorable only to a certain extent, that is, 50% of the total capacity of NN, beyond which it makes the O-sites energetically unfavorable for H absorption. Plots of E_O for three sites with, that is, NN = 0 and NNN = 0; NN = 0 and NNN = 4; NN = 4 and NNN = 0 for PdAg and PdAu alloys are shown in parts d and e of Figure 3, respectively. For a PdAg alloy, in all cases, the sites with NN = 0, NNN = 0, and NN = 0, NNN = 4 are always energetically favorable sites for H absorption. In addition, they become more favorable with increasing Ag content. However, for the O-site with local composition NN = 4, NNN = 0, E_O decreases until the alloy composition is about 25.93% Ag and continues to decrease thereafter. It becomes energetically unfavorable for 37.04% and 48.15% Ag. The situation is slightly different for PdAu alloys, in that all of these sites are favorable over the range of alloy compositions, from 0 to 37% Au.

The effect of the local alloy composition on the O-site binding energy of PdAg, PdAu, and PdCu alloys is shown in a 3D plot in Figures 4−6. The PdAg alloys with 14.81%, 25.93%, 37.04%, and 48.15% Ag, PdAu alloys with 14.81%, 25.93%, and 37.04% Au, and PdCu alloys with 25.93% and 48.15% Cu are shown. It can be seen from Figure 4a that with a 14.81% Ag composition in a PdAg alloy that O-site binding energies in the structure do not have significant differences and are energetically favorable for H adsorption to the same extent. The maximum O-site binding energy is observed as 0.068 eV for NN = 4 and NNN = 0, with a minimum of −0.18 eV at NN = 0 and NNN = 0. The majority of the sites are energetically favorable indicating that H absorption will occur at these sites. However, at 25.93% Ag composition in PdAg alloy, the results

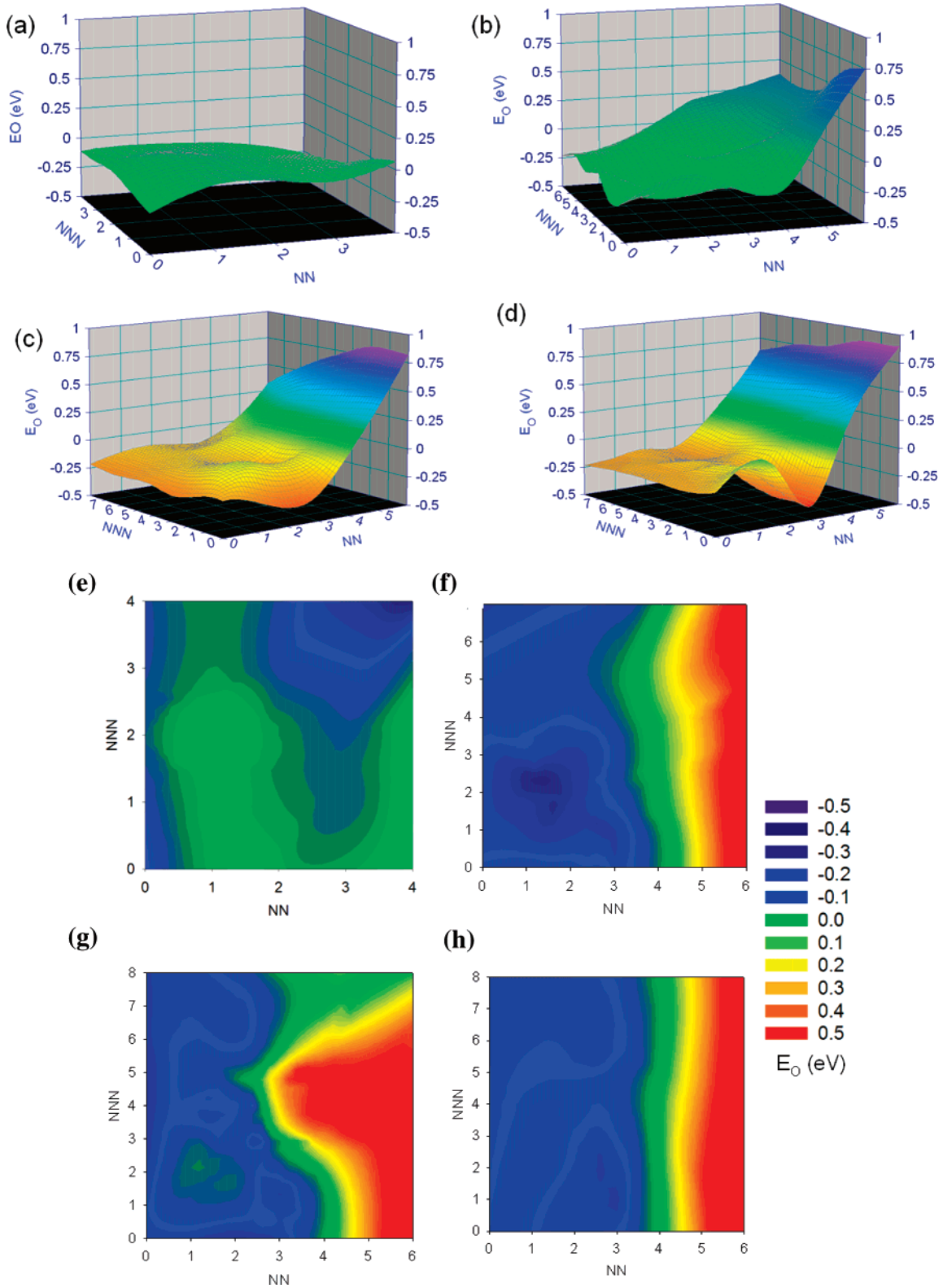

Figure 4. 3-D mesh and 2-D contour plots of O-site binding energies of PdAg alloy as a function of NN and NNN for (a)/(e) 14.81, (b)/(f) 25.93, (d)/(g) 37.04, and (d)/(h) 48.51% Ag.

are significantly different. There are several sites which are energetically favorable while few are energetically unfavorable sites, that is, exhibit high binding energies. The minimum O-site binding energy is observed at −0.288 eV for NN = 2 and NNN = 2, with a maximum at 0.756 eV for NN = 6 and NNN = 0. All the sites with NN > 4 are energetically unfavorable, having a positive binding energy. All the sites with Ag atoms in the NNN shell and NN < 4 create energetically favorable binding sites. The PdAg alloy with a 37.04% Ag composition has stronger O-sites as compared to those observed in PdAg alloys with 25.93% Ag and 14.81% Ag compositions. In addition, it has more favorable O-sites as compared to the alloy with 25.93% Ag. For the PdAg alloy 48.15% Ag, all of the O-sites with local alloy composition of NN > 3 are energetically unfavorable. Here as well, the presence of Ag atoms in the NNN shell makes the O-site energetically favorable for H binding. However, the

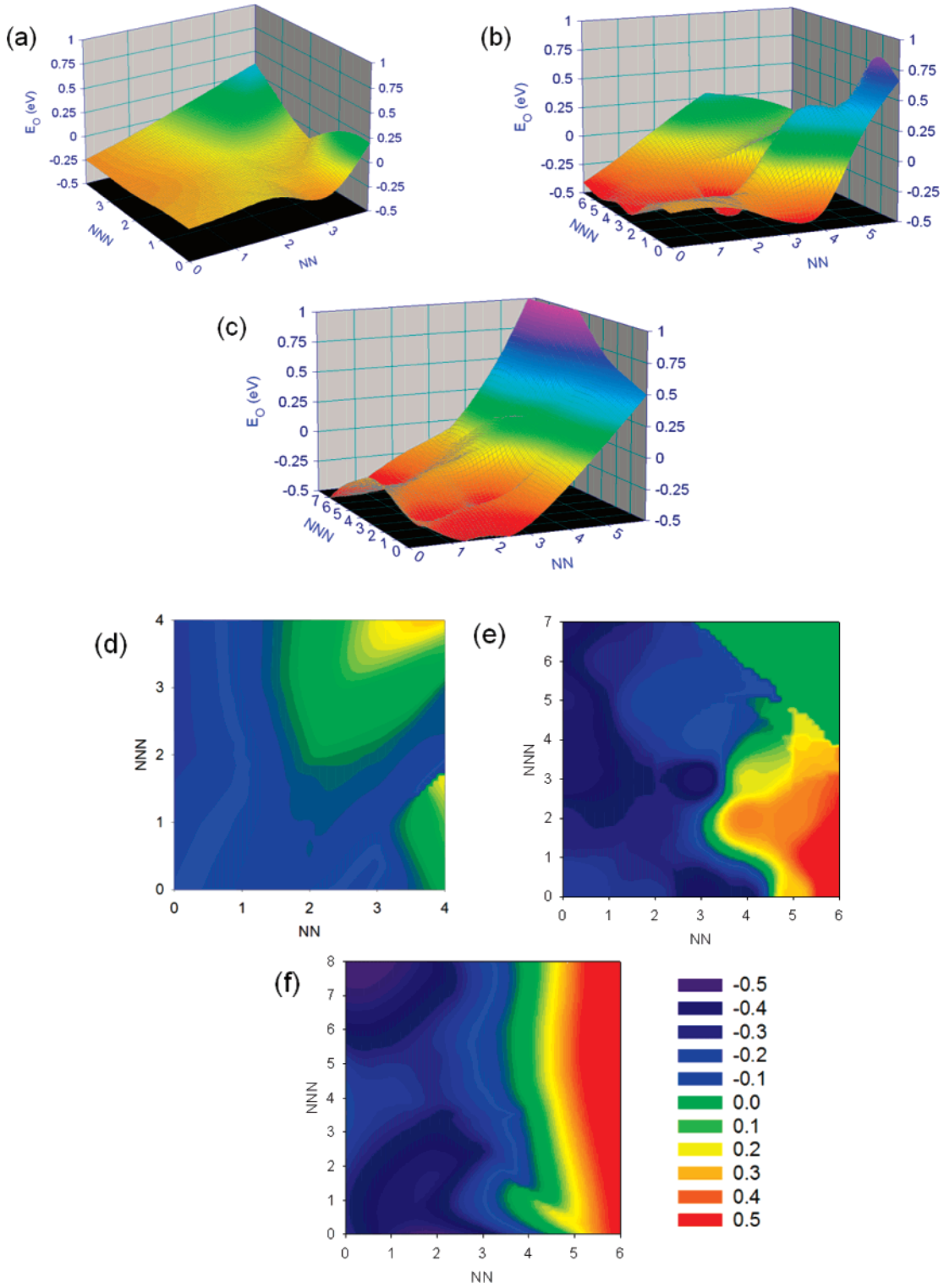

Figure 5. 3-D mesh and 2-D contour plots of O-site binding energy PdAu alloy as a function of NN and NNN for (a)/(d) 14.81, (b)/(e) 25.93, and (c)/(f) 37.04% Au.

number of energetically unfavorable O-sites is more than the alloy with 25.93% Ag. The purpose of gaining several O-site binding energies was to develop a model for representing the classical O-site energies in a form that can be used to estimate the binding energy of any alloy in the range of 0−50% Ag of which O-sites can be identified by means of NN and NNN and the lattice constant. This methodology will help us to identify the alloy composition in which the solubility lies at a maximum. The binding energy data for all four alloys was combined to fit a nonlinear equation given by eq iii,

$$E_O = a_1 + a_2 n_{NN} + a_3 n_{NNN} + a_4 a_0 + a_5 n_N Nn_{NNN} + a_6 n_{NN} a_0 + a_7 n_{NNN} a_0 + a_8 n_{NN}{}^2 + a_9 n_{NNN}{}^2 + a_{10} a_0{}^2 \quad \text{(iii)}$$

where a_0 is the lattice constant, n_{NN} and n_{NNN} are the nearest and next nearest neighboring alloying atoms (Ag, Au, or Cu), respectively, and the coefficients a_1−a_{10} for PdAg, PdAu, and PdCu are summarized in Table 4. As discussed earlier, we have

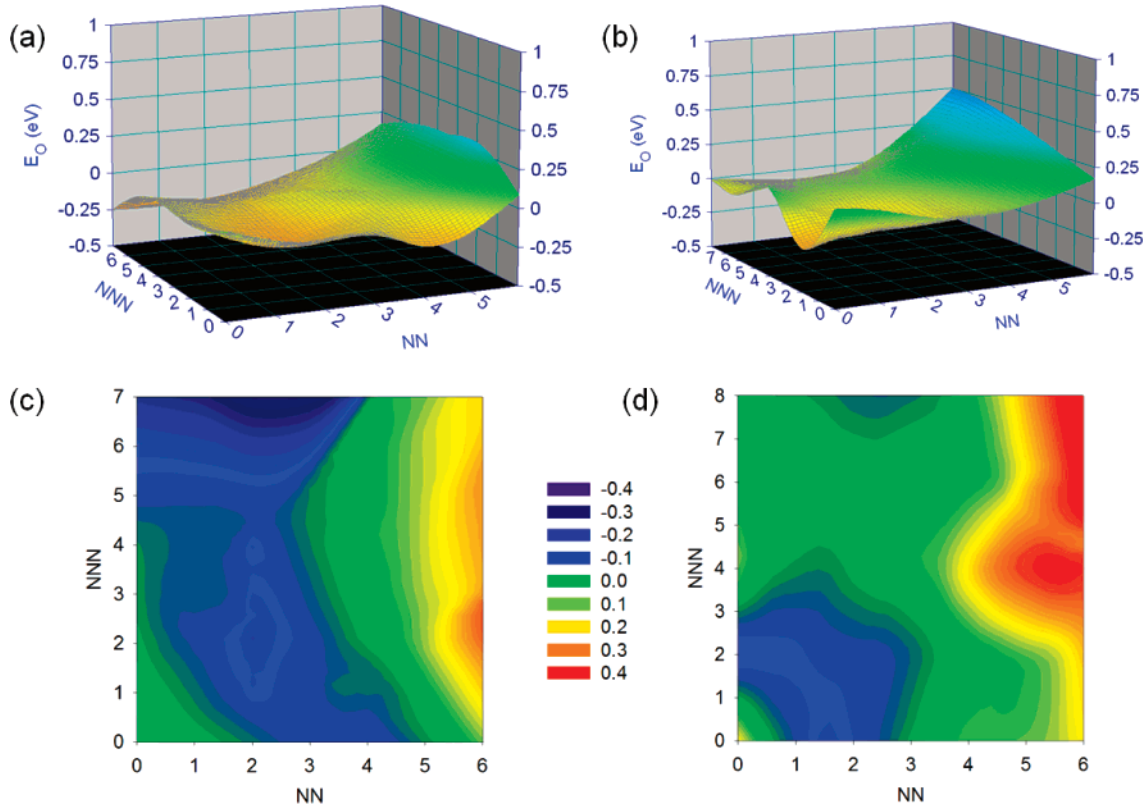

Figure 6. 3-D mesh and 2-D contour plots of O-site binding energy PdCu alloy as a function of NN and NNN for (a)/(c) 25.93 and (b)/(d) 48.51% Cu.

TABLE 4: Constants for PdAg, PdAu, and PdCu Alloys Used in eq iii

constants	PdAg	PdAu	PdCu
a_1	-2.318×10	8.132×10	1.049×10^{-1}
a_2	-2.099×10^{-1}	1.581×10	7.423×10^{-1}
a_3	$-4.373 \times 10^{+2}$	$-1.387 \times 10^{+3}$	8.196×10^{-2}
a_4	$8.862 \times 10^{+2}$	$2.795 \times 10^{+3}$	5.740×10^{-1}
a_5	-1.413×10^{-3}	2.195×10^{-2}	1.020×10^{-2}
a_6	5.623×10^{-2}	-3.931×10^{-1}	-1.937×10^{-1}
a_7	5.497×10^{-1}	-2.062×10	-5.673×10^{-2}
a_8	4.2×10^{-2}	5.420×10^{-2}	2.207×10^{-2}
a_9	-2.096×10^{-3}	-3.560×10^{-3}	-2.017×10^{-3}
a_{10}	$5.394 \times 10^{+1}$	$1.722 \times 10^{+2}$	-5.727×10^{-2}

used the estimates of DFT-based O-site binding energy obtained from a single supercell to obtain a model O-site binding energy for a larger alloy. A comparison of model and classical O-site binding energy of PdAg, PdAu, and PdCu alloys is shown in Figure 7. It can be seen that the model O-site binding energy is close to the DFT-based classical binding energy, with the maximum difference between the two at −0.098 eV. The O-site binding energy is a strong function of NN and a weaker function of NNN. Small irregularities on the plot in Figures 4−6 could be attributed to the arrangement of atoms in the NN or NNN shell. It should be noted that the maximum values for NN and NNN are 6 and 8, respectively. Therefore, for instances such as NN = 3 atoms, the location of these 3 atoms in the 6 possible locations around the O-site could lead to a small difference in the binding energies. As much as a 5−10% difference in binding energies was observed for the same number of alloying atoms in NN and NNN shells but with a different location. Each Ag atom in an NN shell can occupy 6 sites; similarly, 2 atoms can occupy any 2 sites out of the possible 6 sites and so on. Depending upon the location of these atoms, that is, either adjacent or diagonally opposite, the binding energy of the O-site could be different.

4. Solubility of H in PdCu, PdAg, and PdAu. The main goal of the present work is to predict the solubility of a binary alloy of Pd with Ag and Au where the overall alloy composition could range between 0 and 100% of the alloying metal over a broad range of temperatures. The procedure for the simulation of an alloy and the method of estimating solubility of H in the alloy was an extension of the work by Kamakoti et al.[4] who simulated the PdCu system. Therefore, we have estimated the solubility of H in the PdCu system and compared it with their simulations. The solubility of H in the PdCu, PdAg, and PdAu alloy system is shown in Figure 8. The $P-T$ plots for the H concentration of 3.7% in PdAg and PdAu alloys are shown in Figure 9. As seen from Figure 8a, the solubility of H in the PdCu alloy is lower than that of pure Pd. The solubility results by the present method match closely with the experimental data while the simulations reported by Kamakoti et al.[2] underpredict the solubility at higher temperatures for both pure Pd as well as 20% Cu alloys. A comparison of the solubility of H in PdAg alloy at 456, 590, 691, and 1095 K for a broad range of alloy composition from 0 to 50% Ag is shown in Figure 8c. Our model overpredicts the solubility of H in a PdAg alloy at 456 K in the 20−40% Ag range. However, for higher temperatures, that is, 590, 691, or 1095 K, the predicted solubility matches closely with experimental data.[25] There have been conflicting reports in the literature with regards to solubility data. In pioneering work, Gryaznov[6] found that the solubility of H in PdAu system is higher than pure Pd and for some compositions, even higher than that for the PdAg system. However, others such as Grashoff et al.[26] found that solubility of PdAu is significantly low. One of the reasons for lower solubility could be nonuniform distribution of Au in Pd alloy while making the membrane making some pockets with higher Au and some with no Au metals.

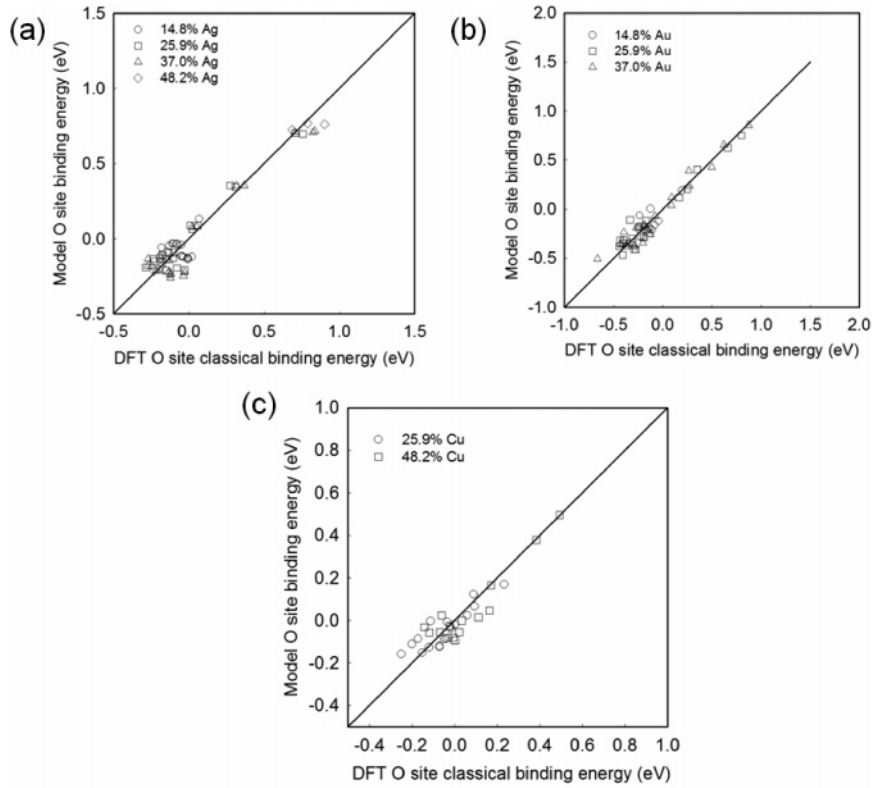

Figure 7. Comparison of classical DFT binding energy vs the model O-site binding energy for (a) PdAg, (b) PdAu, and (c) PdCu alloys.

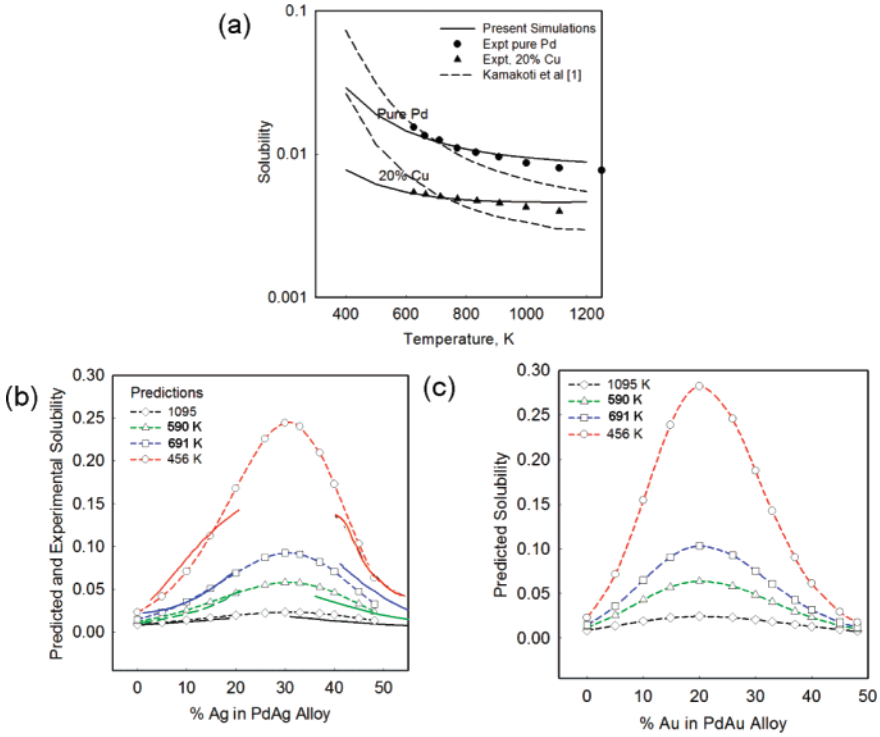

Figure 8. Solubility of H in (a) PdCu, (b) PdAg (experimental data taken from Knapton[25] is shown by solid line), and (c) PdAu alloys.

However, the stronger binding sites in PdAu are expected to give higher solubility in PdAu as compared to PdAg alloys. The predicted solubility of H in PdAu alloys at 456 K, 590, 691, and 1095 K is shown in Figure 8c. It can be seen from parts b and c of Figure 8 that the solubility of H in PdAg and PdAu alloys at a given temperature increases with increasing alloying metal concentration (Ag or Au) and reaches a maximum and decreases thereafter. For example, the solubility of H in a PdAg alloy at 456 K and 30% Ag is about 10 times higher than that of pure Pd. Similarly, the solubility at 590 K is 6 times higher than that of pure Pd. For other temperatures, that is, 691 and 1095 K, the solubility of H in the same alloy is 5 and 3 times higher than that of pure Pd, respectively. The maximum of solubility was always found to occur around 30% Ag in PdAg alloys. The solubility of PdAu alloys shown in Figure 8c also exhibits a similar trend, except that the solubility for the given temperature and composition is higher than the PdAg system and that the maximum solubility occurs around 20% Au. The

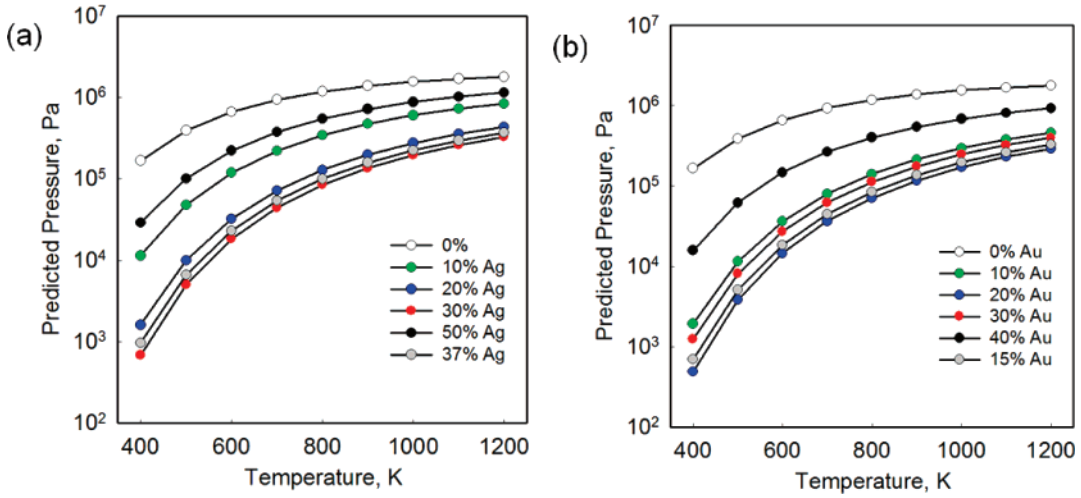

Figure 9. *P*−*T* plot for various (a) PdAg and (b) PdAu alloys.

solubility of H at 456 in PdAu with 20% Au is about 12 times higher than that of pure Pd. This can be compared with the corresponding PdAg system where the solubility of the PdAg system is 10 times higher than pure Pd. The maximum solubility for PdAu at 590, 691, and 1095 K is 7, 5, and 3 times higher than that of pure Pd, respectively.

The *P*−*T* plots for the PdAg and PdAu systems for 0−50% alloying metal concentration and over 400−1200 K are presented in parts a and b of Figure 9, respectively. At a given temperature, for achieving a concentration of 3.7% H in PdAg alloys, the pressure required is much lower than when compared to that of pure Pd. For example, for a PdAu alloy with 20% Au at 600 K, it requires 14.58 kPa to achieve 3.7% concentration of H. However, for a similar situation such as the case of the PdAg alloy, it would require 32.02 kPa. This indicates the favorable energetics offered by the PdAu structure with 20% Au as compared to PdAg alloys.

Conclusions

It was found that DFT overpredicts the lattice constant for PdAg and PdAu alloys over the experimental results by about 2−3%. The lattice expansion of pure Pd and its alloys at low H should not be ignored since it plays a significant role in the solubility predictions. In one of the representative O-sites, by ignoring cell expansion due to H addition, the binding energy was found to be affected by 3.56% with the solubility being affected by 11.8%. The predicted lattice expansion over a range of H concentrations was found to be within 2% of experimental values. The solubility of H in a PdAg or PdAu alloy is higher than that of pure Pd, and the PdAg alloy exhibits a maximum solubility at 30% Ag while the PdAu shows maximum solubility at 20% Au. The estimates of solubility for PdAg (30% Ag at 456 K) are 10 times that of pure Pd. For PdAu (20% Au at 456 K) alloys, the solubility was found to be 12 times higher than that of pure Pd. The simulated solubility of PdAg alloys match closely with the experiments at high temperatures (590 K or higher). At low temperature (456 K), the predicted solubility of PdAg is 1.25 times higher than the experimental value. The solubility of PdCu is lower than PdAg as well as PdAu alloys. A detailed investigation of binding energy as a function of NN and NNN (nearest and next nearest neighbors) suggested that in an alloy several O-sites have significantly higher (positive) binding energies, making it energetically unfavorable for H absorption. Also, in several cases, the T-site is energetically favorable for H absorption as compared to an adjacent O-site. Overall, by either having low NN (number of alloying atoms in NN shell), or having higher NNN in the local alloy composition produces energetically favorable O-sites. In summary, the DFT-based simulations can be used to design Pd alloy membranes with higher H solubility.

Acknowledgment. We acknowledge the Shell International Exploration and Production Inc. and Shell Hydrogen for financial support and Mr. Josh Brandt for assistance in the computational resources.

References and Notes

(1) Wicke, W.; Brodowsky, H. *Hydrogen in Metals 2*; Alefeld, G., Volkl, J., Eds.; Springer-Verlag: Berlin, 1978; p 73.
(2) Kamakoti, P.; Morreale, B. D.; Ciocco, M. V.; Howard, B. H.; Killmeyer, R. P.; Cugini, A. V.; Sholl, D. S. *Science* **2005**, *307*, 569.
(3) Kamakoti, P.; Sholl, D. S. *J. Membr. Sci.* **2003**, *225*, 145.
(4) Kamakoti, P.; Sholl, D. S. *Phys. Rev. B* **2005**, *71*, 014301-1.
(5) Graham, T. *Proc. R. Soc. London* **1869**, *17*, 212.
(6) Gryaznov, V. M. *Sep. Purif. Methods* **2000**, *29*, 171.
(7) Uemiya, S.; Matsuda, T.; Kikuchi, E. *J. Membr. Sci.* **1991**, *56*, 315.
(8) Amandusson, H.; Ekedahl, L.-G.; Dannetun, H. *J. Membr. Sci.* **2001**, *193*, 35.
(9) Gillan, M. J. *J. Phys. C: Solid State Phys.* **1986**, *19*, 6169.
(10) Jemma, N.; Grandjean, B. P. A.; Kaliaguine, S. *Can. J. Chem. Eng.* **1995**, *73*, 405.
(11) Yokoi, Y.; Seki, T.; Yasuda, I. *Advances in H Energy*; Padro, G., Catherine, E., Eds.; Kluwer Academic: 2000; p 111.
(12) Ke, X.; Kramer, G. J. *Phys. Rev. B* **2002**, *6*, 184304.
(13) Løvvik, O. M.; Olsen, R. A. *J. Alloys Compd.* **2002**, 330−332.
(14) Kresse, G.; Hafner, J. *Phys. Rev. B* **1993**, *48*, 13115.
(15) Kresse, G.; Furthmuller, J. *Comput. Mater. Sci.* **1996**, *6*, 15.
(16) Rowe, J. M.; Rush, J. J.; de Graaf, L. A.; Ferguson, G. A. *Phys. Rev. Lett.* **1972**, *29*, 1250.
(17) Nelin, G.; Skold, K. *J. Phys. Chem. Solids* **1975**, *36*, 1175.
(18) Nelin, G.; Skold, K. *J. Phys. Chem. Solids* **1967**, *28*, 2369.
(19) Worsham, J. E.; Wilkinson, C. G.; Shull, M. K. *J. Phys. Chem. Solids* **1967**, *28*, 2369.
(20) Massalski, T. B., Ed. *Binary Alloy Phase Diagram*; American Society for Metals: Metals Park, Ohio, 1986; Vols. 1 and 2.
(21) Fowler, R. H.; Smithells, C. *Proc. R. Soc. London: Ser. A* **1937**, *160*, 37−47.
(22) Wagner, C. *Acta Metall.* **1973**, *21*, 1297.
(23) Pearson, W. B. *A Handbook of Lattice Spacing and Structure of Metal and Alloys*; Pergamon Press: New York, 1967; Vol. 2.
(24) Mealand, A.; Flanagan, T. B. *J. Phys. Chem.* **1911**, *69*, 3537.
(25) Knapton, A. G. *Platinum Met. Rev.* **1977**, *21*, 44.
(26) Grashoff, G. J.; Pilkington, C. E.; Corti, C. W. *Platinum Met. Rev.* **1983**, *27*, 157.